HHS Public Access

Author manuscript

Alzheimers Dement. Author manuscript; available in PMC 2024 November 01.

Published in final edited form as:

Alzheimers Dement. 2023 November ; 19(11): 5185–5197. doi:10.1002/alz.13086.

Retinal arterial $A\beta_{40}$ deposition is linked with tight junction loss and cerebral amyloid angiopathy in MCI and AD patients

Haoshen Shi[1], **Yosef Koronyo**[1], **Dieu-Trang Fuchs**[1], **Julia Sheyn**[1], **Ousman Jallow**[1], **Krishna Mandalia**[1], **Stuart L. Graham**[2], **Vivek K. Gupta**[2], **Mehdi Mirzaei**[2], **Andrei A. Kramerov**[3], **Alexander V. Ljubimov**[1,3,4], **Debra Hawes**[5], **Carol A. Miller**[5], **Keith L. Black**[1], **Roxana O. Carare**[6], **Maya Koronyo-Hamaoui**[1,4,7,⌘]

[1]Department of Neurosurgery, Maxine Dunitz Neurosurgical Research Institute, Cedars-Sinai Medical Center, Los Angeles, CA 90048, USA

[2]Macquarie Medical school, Faculty of Medicine, Health and Human Sciences, Macquarie University, Sydney, NSW 2109, Australia.

[3]Department of Biomedical Sciences and Eye Program, Board of Governors Regenerative Medicine Institute, Cedars-Sinai Medical Center, Los Angeles, CA 90048, USA

[4]Department of Biomedical Sciences, Division of Applied Cell Biology and Physiology, Cedars-Sinai Medical Center, Los Angeles, CA 90048, USA

[5]Department of Pathology Program in Neuroscience, Keck School of Medicine, University of Southern California, Los Angeles, CA 90048, USA

[6]Department of Clinical Neuroanatomy, University of Southampton, Southampton SO16 6YD, UK

[7]Department of Neurology, Cedars-Sinai Medical Center, Los Angeles, CA 90048, USA

Abstract

INTRODUCTION: Vascular amyloid β-protein (Aβ) deposits were detected in retinas of mild cognitively impaired (MCI) and Alzheimer's disease (AD) patients. We tested the hypothesis that the retinal vascular tight junctions (TJs) were compromised and linked to disease status.

⌘Corresponding author: Maya Koronyo-Hamaoui, PhD, Cedars-Sinai Medical Center, 127 S. San Vicente Blvd., Los Angeles, CA 90048, USA. Tel: (310)-423-7473, maya.koronyo@csmc.edu.

Author contributions: H.S. designed and performed experiments, collected, and analyzed data, created figures, drafted, and edited the manuscript. Y.K. performed experiments and collected data. D.F. performed experiments and drew the illustration graph. J.S. analyzed data and created figures for proteomic analysis. O.J. performed experiments. V.K.G., S.L.G. and M.M. performed retinal proteomic analysis, analyzed data, and provided methods. A.V.L. and A.A.K. provided donor eyes and clinical reports and edited the manuscript. K.L.B. assisted with data interpretation and manuscript editing. R.O.C. provided study conception and interpretation, illustration of intramural peri-arterial drainage system, and edited the manuscript. M.K.H. was responsible for study conception and design, data analysis and collection, interpretation of data, study supervision, and manuscript writing and editing. All authors have read and approved of this manuscript.

Conflict of interest: Y.K., M.K.H., and K.L.B. are co-founders and stockholders of NeuroVision Imaging, Inc., Sacramento, CA, USA. H.S., D.F., J.S., O.J., K.M., S.L.G., V.K.G., M.M., A.A.K., A.V.L., D.H., C.A.M. and R.O.C. declare no potential conflicts of interest.

Consent statement: This study is not considered a human subjects research and we confirm that consent was not necessary, for the reasons described as follow: we processed and analyzed deidentified retinal tissues of deceased patients that were provided by the USC-ADRC (C.A.M, D.H.) and from the NDRI (A.V.L.).

METHODS: TJ components and Aβ expression in capillaries and larger blood vessels were determined in postmortem retinas from 34 MCI or AD patients and 27 cognitively normal controls, and correlated with neuropathology.

RESULTS: Severe decreases in retinal vascular zonula occludens-1 (ZO-1) and claudin-5 correlating with abundant arteriolar $A\beta_{40}$ deposition were identified in MCI and AD patients. Retinal claudin-5 deficiency was closely associated with cerebral amyloid angiopathy, whereas ZO-1 defects correlated with cerebral pathology and cognitive deficits.

DISCUSSION: We uncovered deficiencies in blood-retinal barrier markers for potential retinal imaging targets of AD screening and monitoring. Intense retinal arteriolar $A\beta_{40}$ deposition suggests a common pathogenic mechanism of failed Aβ clearance via intramural periarterial drainage.

Keywords

Blood-retinal barrier; amyloid angiopathy; retinopathy; Alzheimer's disease

1. BACKGROUND

Small blood vessel abnormalities and cerebral amyloid angiopathy (CAA) are the most frequently identified vascular pathologies in Alzheimer's disease (AD)[1]. More than 85% of AD patients display varying severity of CAA[2,3]. The Aβ species present within CAA in AD brains primarily consists of the 40-amino acid amyloid β-protein ($A\beta_{40}$) alloforms that are predominantly deposited in the tunica media and adventitia of leptomeningeal and cerebral parenchymal arteries[4]. The failure of Aβ clearance via the intramural peri-arterial drainage (IPAD) pathway is key to the pathogenesis of CAA, leading to neuronal, and homeostatic dysfunctions in the brain, often associated with worsen cognitive impairments[5,6]. Another crucial mechanism correlated with insufficient clearance of cerebral vascular Aβ is blood-brain barrier (BBB) breakdown. Recent findings suggest that early BBB dysfunction and cerebral vascular damage frequently occur before brain neuropathology and cognitive decline are recognized[7].

The retina, an anatomical extension of the brain dating back to the embryonic stage, has been extensively examined as a possible window to central nervous system (CNS) disorders[8-10]. Along with recent progress in retinal amyloid imaging, hyperspectral imaging, fundoscopy, and optical coherence tomography-angiography in AD patients[11-16], the retina has become a new direction for early or pre-symptomatic AD screening at high spatial resolution and specificity. To date, a broad array of AD pathologies have been demonstrated in the retinas of mild cognitive impairment (MCI) and AD patients, including vascular dysfunctions, gliosis, Aβ plaques and vascular $A\beta_{40}$ and $A\beta_{42}$ deposits, abnormal tau accumulation, and neurodegeneration[8,11,12,14,17-22]. Our recent work in retinas from patients with MCI and AD dementia revealed early and progressive pericyte loss along with vascular Aβ accumulation; these were associated with the severity of brain-regional Aβ plaque, CAA, and cognitive deficit[23]. Another study described a significant increase in retinal capillary blood flow and flow heterogeneity in early-stage autosomal dominant AD carriers compared to controls. This suggests the existence of potential functionally

relevant retinal vascular biomarkers that may be specific to AD pathogenesis[24]. In retinas of double transgenic $APP_{SWE}/PS1_{\Delta E9}$ AD-model mice, we also discovered age-dependent accumulation of vascular $A\beta_{40}$, capillary loss, tight junction (TJ) degeneration, and blood-retinal barrier (BRB) leakage, compared to retinas of wild-type healthy controls[25]. These intriguing discoveries lead to the hypothesis that BRB is disrupted in AD patients and it relates to retinal vascular Aβ deposition, cerebral pathology, and cognitive decline.

Here we investigated the expression patterns of endothelial TJ components and vascular amyloidosis in capillaries, arteries, and veins in postmortem retinas from a cohort of 10 MCI, 24 AD patients and 27 cognitively normal (CN) controls. We identified novel retinal vascular markers that may predict the development of CAA and cognitive decline related to AD.

2. METHODS

Extended methods are provided in Supplementary Materials.

2.1 Sources of postmortem eyes

Eyes from deceased AD and MCI patients and CN controls (n=61 subjects) were obtained from the University of Southern California Alzheimer's Disease Research Center (USC-ADRC) Neuropathology Core (IRB-HS-042071) and the National Disease Research Interchange (NDRI, Philadelphia, PA) under Cedars-Sinai Medical Center IRB-Pro00019393. Clinical and neuropathological data are detailed in Tables 1 and 2 and Supplementary Table 1.

2.2 Clinical and neuropathological assessments

The USC-ADRC Clinical Core provided records of neurological examinations and cognitive evaluations as well as extensive brain pathology reports.

2.3 Processing of eyes and preparation of retinal cross-sections and vascular network for immunostaining

Donor eyes were collected, preserved, and processed for analysis. Retinal cross-sections from superior-temporal geometric subregions were prepared for histological analyses by immunostaining. Information on the antibodies used is provided in Supplementary Table 2. Retinal vascular networks were isolated from retinal flat mounts and immunostained as previously described[23].

2.4 Microscopy and stereological quantification

Quantitation of retinal vascular claudin-5, ZO-1, and $A\beta_{40}$ in NIH Image J was performed on microscopic images captured using fluorescence and a bright-field Carl Zeiss Axio-Imager Z1 microscope with ZEN 2.6 blue edition software. On average, 12 images (20× magnification) were obtained from each patient for quantification (see details in Supplementary Methods).

2.5 Proteome analysis using mass spectrometry

This analysis included the following: a) preparation of retinal homogenates; b) TMT labelling; c) nanoflow liquid chromatography electrospray ionization tandem mass spectrometry; d) database searching, peptide quantification, and statistical analysis; and e) functional network and computational analysis. The mass spectrometry proteomics data have been deposited to the ProteomeXchange Consortium via the PRIDE[26] partner repository with the dataset identifier PXD040225.

2.6 Statistical Analysis

GraphPad Prism Software version 8.3.0 was used for analyses. One- or two-way ANOVA followed by Tukey's multiple comparison post-test and two-tailed unpaired Student's t-test were used to analyze statistical significance between groups. Pearson's correlation coefficient (r) test was used to determine associations between markers in this study.

3. RESULTS

3.1 Retinal endothelial claudin-5 deficiency in MCI and AD patients is strongly linked to CAA severity

Claudin-5 is an essential TJ component that connects endothelial cells within the BRB and BBB. Downregulation of vascular endothelial claudin-5 was implicated in both neurodegenerative disorders and retinal vascular diseases, leading to disruption and leakage of the BBB or BRB[27,28]. Here, we isolated postmortem retinas and prepared retinal cross-sections from a cohort of patients with MCI (n=10, mean age 88.7 ± 5.7 years, 6 females/4 males), AD (n=21, mean age 85.6 ± 8.5 years, 11 females/10 males), and CN controls (n=22, mean age 82.1 ± 10.9 years, 11 females/11 males). There were no significant differences in mean age, sex, or post-mortem interval (PMI) between the three diagnostic groups (see Tables 1 and 2, and Supplementary Table 1 for more details).

3.1.1 Marked loss of retinal endothelial claudin-5 in capillaries and large blood vessels (LBVs) of patients with CAA pathology—Claudin-5 expression in both capillaries and LBVs was determined by immunostaining followed by stereological quantification of the immunoreactive area (IR) in prepared retinal cross-sections from this cohort (Fig. 1; female vs. male data in Supplementary Fig. 1a-b). Collagen IV (ColIV) was co-stained with claudin-5 to visualize retinal blood vessels (Fig. 1a). We noticed a progressive loss of retinal vascular claudin-5 with increased CAA severity scores in all patients, regardless of diagnostic group (Fig. 1a); Interestingly, prominent expression of claudin-5 was present in both retinal capillaries and LBVs in AD patients with CAA severity score 0, whereas in those with CAA score 2 most retinal vascular claudin-5 expression was lost. Quantification of retinal vascular claudin-5 revealed significant decreases in capillary and LBV claudin-5 expression in patients with CAA scores 1-1.5 versus those with CAA score 0 as well as in patients with CAA score 2 versus those with CAA scores 1-1.5 (Fig. 1b). When we compared expression of retinal vascular claudin-5 among different diagnostic groups, we found significant deficiencies in both the capillaries and LBVs of MCI and AD patients compared to CN controls (Fig. 1c). No sex-related differences were noted for retinal vascular claudin-5 expression (Fig. 1d, Supplementary Fig. 1a-b).

3.1.2 Retinal capillary claudin-5 expression is strongly linked to CAA severity and weakly correlates with Braak stage and ABC and Clinical Dementia Rating (CDR) scores in MCI and AD patients.—

Highly significant and strong associations (P<0.0001, r=0.67-0.75) were identified between retinal claudin-5 expression and CAA severity scores in both capillaries and LBVs in a subset of human donor cohorts with neuropathological reports (n=38; Fig. 1e-f). Claudin-5 expression in retinal capillaries, but not in LBVs, was also significantly correlated with cognition according to CDR scores, Braak staging, and A (Thal-A) B (Braak-B) C (CERAD-C) average scores (Fig. 1f).

3.1.3 Correlations between expressions of retinal vascular claudin-5 and $A\beta_{40}$—

Pearson's (r) correlation analysis indicated a significant association between retinal claudin-5 and $A\beta_{40}$ deposition in capillaries (Fig. 1g), with a more significant and much stronger correlation between retinal arteriolar $A\beta_{40}$ and claudin-5 in LBVs (Fig. 1h).

3.2 Early and prominent downregulation of retinal vascular ZO-1 in MCI and AD patients correlates with cerebral pathology and cognitive deficit

TJ protein ZO-1 is an essential component that builds the link of transmembrane TJ proteins claudins and occludins with the actin cytoskeleton[29,30]. We previously found significant ZO-1 downregulation in retinas of AD-model mice[25]. Here we investigated expression of ZO-1 in correlation with retinal vascular amyloidosis, cerebral pathology, and cognitive decline.

3.2.1 Decreased ZO-1 expression along with $A\beta_{40}$ deposition in isolated retinal blood vessels—

We previously described a modification of the established enzymatic retinal vascular isolation technique[31,32] to immunofluorescence-based staining and stereological quantification analyses[23,25]. In the current study, we isolated retinal blood vessels from an AD patient with moderate CAA severity (score 1.5) and an age- and sex-matched CN control with no known CAA pathology (Fig. 2a-b). There was substantial loss of cellular ZO-1 and intense vascular $A\beta_{40}$ deposition in the retina of the AD patient versus the control; this was especially apparent in small retinal capillaries (Fig. 2a-b, right panels).

3.2.2 Downregulation of retinal ZO-1 and upregulated inflammatory pathways in AD patients—

In a different cohort of AD human donors (n=6, mean age 82.5 ± 19.4 years, 4 females/2 males) and CN controls (n=6, mean age 76.8 ± 5.9 years, 3 females/3 males), we processed postmortem retinas for protein lysates to perform bulk proteomic analyses using mass spectrometry (Fig. 2c-d). The analysis revealed global downregulation of vascular biomarkers including ZO-1, smoothelin, and vascular endothelial zinc finger 1 (VEZF1) in the retinas of AD donors compared to controls (Fig. 2c). Intriguingly, we also found upregulation of inflammatory and leukostasis biomarkers CD11b and integrin subunit beta 2 (Itgb2). Moreover, canonical pathway analyses of mass spectrometry data using Ingenuity Pathway Analysis (IPA) software suggested upregulation of several signaling pathways including interleukin (IL)-1, IL-6, IL-8, integrin, and vascular endothelial growth factor (VEGF), and remodeling of epithelial adherens junctions (Fig. 2d).

3.2.3 Loss of retinal vascular ZO-1 in early functional impairment and AD dementia is moderately correlated with cerebral pathology and cognitive decline—

We next investigated the expression of retinal vascular ZO-1 in both capillaries and LBVs in the cohort shown in Table 1 (Fig. 2e-i, Supplementary Fig. 1c-d, Supplementary Fig. 2). In both capillaries and LBVs, early and substantial degeneration of ZO-1 was observed in MCI and AD patients, with severe retinal vascular $A\beta_{42}$ deposition that was mostly seen in AD patients (Fig. 2e-f, Supplementary Fig. 2a-c). Quantification of vascular ZO-1 demonstrated this early downregulation in both capillaries and LBVs from MCI patients versus CN controls (Fig. 2g). Donors with CAA pathology (severity scores ≥ 1) displayed significantly less retinal vascular ZO-1 expression in both capillaries and LBVs compared to donors with CAA severity scores < 1 (Fig. 2h-i). ZO-1 expression in capillaries and LBVs was inversely associated with retinal vascular $A\beta_{40}$ burden (Fig. 2h-i). No sex-related difference was found in ZO-1 expression in either type of retinal blood vessels (Supplementary Fig. 1c-d).

3.2.4 Significant correlation between retinal vascular ZO-1 deficiency and severity of brain AD pathology and cognition—

In a subset of human donor cohort with neuropathological reports (n=38), retinal vascular ZO-1 expression in both capillaries and large blood vessels was significantly and moderately associated with a wide spectrum of AD-related cerebral pathology, including neurofibrillary tangles (NFT), neuropil threads (NT), CAA, Braak stages, and ABC scores (Fig. 2j). Overall, the associations between retinal capillary ZO-1 expression and brain pathologies were stronger than those between LBV ZO-1 and brain pathologies, whereas capillary ZO-1 reflected more strongly NFT scores. Note that CDR-determined cognitive function also correlated with retinal vascular ZO-1.

3.3 In retinas of MCI and AD patients, more $A\beta_{40}$ is accumulated in arterioles than in venules, and retinal arteriolar $A\beta_{40}$ is tightly associated with CAA scores

Since we found a strong association between retinal vascular TJ loss and Aβ deposition, we sought to investigate $A\beta_{40}$ accumulation in each retinal vascular subtype (capillary, arteriole, and venule) and determine in which type(s) of retinal blood vessel vascular $A\beta_{40}$ may drive TJ disruption and predict brain neuropathology.

3.3.1 Retinal vascular $A\beta_{40}$ deposition accumulates mostly in arterioles—

In a different donor cohort of MCI (n=8), AD (n=15), and CN controls (n=15), we immunostained retinal cross-sections for 11A50-B10 antibody[23] to examine the $A\beta_{40}$ burden in different types of retinal blood vessels. Nomarski microscopy together with staining for α-smooth muscle actin (α-SMA) and ColIV, along with $A\beta_{40}$, differentiated between blood vessel types: ColIV detects the basement membrane of all types of blood vessels; α-SMA identifies smooth muscle cells and, thereby, can be used to separate between arteries/arterioles and veins/venules based on the continuity and layers of $\alpha\text{-SMA}^+$ cells [6]. In the retinal cross-sections that we prepared, retinal arterioles and venules were mostly seen instead of larger arteries and veins. Immunostaining of $A\beta_{40}$ in an AD patient with CAA severity score 2 revealed strong retinal arteriolar $A\beta_{40}$ deposition in the tunica media and tunica adventitia and inside smooth muscle cells (Fig. 3a, Supplementary Fig.

3a). In the same patient, there is less $A\beta_{40}$ accumulated in retinal capillaries and it is only mildly detected in venules (Fig. 3b, Supplementary Fig. 3b). Retinal arteriolar $A\beta_{40}$ deposition was also observed in MCI patients, but barely detected in CN controls (Fig. 3c-d). However, $A\beta_{40}$ was detected in both retinal arterioles and capillaries from one CN control with CAA severity score 1, (Supplementary Fig. 3c).

Stereological quantification revealed a significant increase in $A\beta_{40}$ in retinal capillaries, arterioles, and venules from AD patients versus CN controls (Fig. 3e). Notably, retinal capillary $A\beta_{40}$, but not arteriolar or venular $A\beta_{40}$, was substantially increased in MCI patients compared to CN controls (Fig. 3e). $A\beta_{40}$ burden was greater in retinal arterioles than in venules and capillaries in all AD patients (Fig. 3f) and in all patients with CAA severity scores ≥ 1 (Fig. 3g). There was a significant difference in $A\beta_{40}$ levels in retinal arterioles, but not capillaries or venules, in patients with CAA severity scores ≥ 1 compared to those with CAA severity scores < 1 in this cohort (Fig. 3g). Additional immunostaining for $A\beta_{40}$ using a different antibody JRF/c$A\beta_{40/28}$ also demonstrated strong accumulation of $A\beta_{40}$ in the tunica adventitia and smooth muscle cells of a retinal arteriole from an AD patient (Fig. 3h). To evaluate if the retinal capillaries of MCI and AD patients exhibit basement membrane (BM) thickening, as observed in patients with diabetic retinopathy (DR)[33], we measured BM thickness in capillaries (≤10μm) labelled with collagen IV or periodic acid/Schiff staining in a subset of 8 AD, 8 MCI and 8 CN individuals. Both analyses showed no differences in retinal capillary BM thickness between the diagnostic groups (Supplementary Fig. 4), suggesting that the effects of AD on retinal vasculature may be different from those of common retinal vascular diseases.

3.3.2 Retinal arteriolar $A\beta_{40}$ deposition strongly associated with CAA severity—

For a subset of donors with neuropathological reports (n=27), Pearson's correlation revealed a strong and significant association between retinal arteriolar $A\beta_{40}$ deposition and CAA severity scores (Fig. 3i, $P<0.0001$, $r=0.77$). CAA was also moderately associated with $A\beta_{40}$ levels in retinal capillaries (Fig. 3i). No other correlations between retinal vascular $A\beta_{40}$ and brain pathology or cognition were found.

4. DISCUSSION

In this study, we identified loss of TJ components in the endothelium of both capillaries and LBVs in postmortem retinas of MCI and AD patients. Downregulation of TJs in both retinal capillaries and larger blood vessels were significantly associated with vascular $A\beta_{40}$ accumulation. Both retinal vascular claudin-5 and ZO-1 deficiencies were significantly correlated with CAA severity scores, whereas retinal capillary claudin-5 strongly reflected CAA severity. Vascular ZO-1 levels were also significantly correlated with a wide spectrum of AD brain biomarkers and cognitive status as measured by CDR but not by Mini-Mental State Examination (MMSE) scores. Global proteomic analysis of AD versus CN control retinas revealed decreased levels of several retinal vascular markers, including ZO-1, along with increased pro-inflammatory pathways that may induce vascular remodeling. Furthermore, intense retinal $A\beta_{40}$ accumulation was observed in arterioles but was far less prevalent in retinal venules and less in capillaries, suggesting a failure of Aβ clearance via IPAD[5,6]. The results of this study uncovered early and substantial retinal vascular

abnormalities in MCI and AD patients that could potentially serve as biomarkers for detecting and monitoring AD as well as CAA severity. Figure 4 illustrates a summary of our findings.

TJs between endothelial cells are essential components of the BBB and inner BRB that are vital for maintaining both cerebral and retinal homeostasis[34-36]. Degeneration of critical TJ molecules claudin-5 and ZO-1 were described in cerebral capillaries of AD patients with CAA and in 5xFAD AD-model mice[37-39]. Our previous studies suggested significant decreases in total levels and vascular expression of ZO-1 and claudin-1 in the retinas of APP/PS1 double transgenic AD-model mice[25,40]. Moreover, we found loss of retinal pericytes and PDGFRβ along with increased retinal vascular amyloidosis in MCI and AD patients, indicating structural and functional alterations in the BRB during AD[23]. Here, we uncovered early loss of both ZO-1 and claudin-5 in retinal blood vessels of MCI patients versus CN controls, which suggests BRB damage appears at the earliest stages of functional impairment in the AD continuum. Strikingly, almost no claudin-5 expression in retinal blood vessels was demonstrated in AD patients with moderate to severe CAA. Such findings indicate a disrupted inner BRB during AD progression. Notably, the association between the extent of retinal TJ loss and the severity of retinal vascular $A\beta_{40}$ deposition was highly significant in this cohort. This indicates a link between BRB damage and vascular amyloidosis that is similar to the association between BBB alterations and CAA found in previous studies[41,42].

Reduction of retinal ZO-1, smoothelin, and VEZF1 in AD patients compared to CN controls is further indicative of disrupted endothelium and smooth muscle cells in the AD retina. Moreover, our results revealed enhanced expression of the pro-inflammatory biomarkers CD11b and Itgb2 among AD patients relative to controls, hinting at augmented retinal leukostasis and inflammation during AD. Further canonical pathway analyses pointed toward upregulations of crucial pro-inflammatory cytokine signaling pathways that could be involved in vascular remodeling and degeneration[43,44]; this includes IL-1, IL-6, IL-8, integrin, and IL-8 signaling pathways. Indeed, previous studies have reported increased cytokine production and microglial activation in the brains of AD patients and animal models[21,40,45,46]. Together with our findings, these data further indicate that retinal inflammation occurs in parallel to brain inflammation in AD. Future investigations should examine these inflammatory and vascular signaling pathways in connection with AD brain pathology and cognitive decline.

Although our previous study found strong deposition of both $A\beta_{40}$ and $A\beta_{42}$ in the retinal blood vessels of AD patients[23], it was unknown which type of blood vessel is mostly affected and associated with cerebral AD pathology. In the current study, retinal vascular $A\beta_{40}$ accumulation in AD patients was predominantly detected in arterioles, especially in patients with moderate to severe CAA. The combination of DIC, α-SMA, and $A\beta_{40}$ microscopic imaging revealed accumulation of arteriolar $A\beta_{40}$ in the vascular tunica media and adventitia layers, in smooth muscle cells, and perivascularly. This finding suggests a compromised IPAD of $A\beta_{40}$ along arterial basement membranes, a main mechanism that contributes to CAA development in the brain[5,6]. Likewise, additional vascular $A\beta_{40}$ deposition exhibited a pattern in retinal arterioles that was very similar to typical CAA

patterns described in the AD brain[47]. Collectively, our data suggest that early vascular amyloidosis occurs in retinal capillaries, becoming more prominent later in arterioles, showing similarities in the development of vascular amyloidosis between the retina and brain in AD.

Among the neuropathological parameters of AD, CAA was most closely associated with retinal vascular markers in this study. In fact, CAA, rather than diagnostic separation by MCI or AD, appears to be a key factor driving retinal vascular claudin-5 loss, since AD patients with CAA score 0 still display strong retinal vascular claudin-5 signals. When we compared all retinal biomarkers, capillary claudin-5 and arteriolar $A\beta_{40}$ were strongly associated with CAA severity (both $P<0.0001$, $r>0.70$). Indeed, these findings warrant future study to investigate the possibilities of monitoring CAA progression by retinal vascular imaging of TJs and amyloid burden. Moreover, ZO-1 expression in retinal capillaries significantly correlated with nearly all cerebral pathologies and cognitive scores as examined in this study; it was associated with cerebral Aβ plaques, NFTs, NTs, CAA, Braak stage, and CDR-determined cognitive status score. Such correlations were found to be more significant and prevalent than what we described between retinal PDGFRβ or vascular $A\beta_{40}$ and cerebral pathology in a previous cohort[23].

We recognize limitations in this study. Although the neuropathological reports of the donor patients included comprehensive data on neurological conditions and brain pathologies, they lacked some information regarding potential confounding factors that may affect data interpretation, including history of diabetes or DR, hypertension, systemic amyloidosis, hereditary transthyretin amyloidosis[48], and other systemic or retinal vascular diseases. Nevertheless, the presence of important AD co-morbidities that were documented in the neuropathological reports, such as Lewy bodies and atherosclerosis, are listed in Supplementary Table 1. Further, although there was no statistical difference between the mean ages of diagnostic groups in the cohorts used for the histological and mass spectrometry analyses, the mean ages of every group are not perfectly matched in our study. In addition, within our cohort, most patients had CAA severity scores that were limited between 0 and 2. Thus, no investigations of retinal TJ integrity in patients suffering from the most severe CAA pathology were performed in this study. Nevertheless, our results did show marked retinal vascular TJ losses in comparison to controls, especially in patients with moderate to severe CAA (scores 1.5-2). This may indicate a high sensitivity of retinal TJs to predict cerebral vascular amyloidosis, with a weaker prediction for cognitive decline in AD patients. Since our cohort is also limited in sample size, future studies with access to severe CAA cases and larger case numbers should be conducted to validate our discoveries. Importantly, although our measurement of retinal capillary BM thickness did not show differences between the study groups, future analysis should be performed using the gold standard test, transmission electron microscopy, to evaluate BM thickness and validate this result.

5. CONCLUSION

In summary, the present study has demonstrated, for the first time, an intense degeneration of claudin-5 and ZO-1 TJs in retinal vasculature that was closely correlated to the severity

of CAA in MCI and AD patients. The strong correlations between retinal vascular ZO-1 expression and a range of cerebral pathology and cognitive decline suggest that ZO-1 could be a potential biomarker for monitoring AD progression. Additionally, our results provide the first evidence of the susceptibility of retinal capillaries to the pathological processes of AD, with enhanced accumulation of $A\beta_{40}$ in retinal arterioles versus venules and strong connections to CAA severity in MCI and AD patients. Combined with previously reported retinal vascular damage in AD patients, such as pericyte loss, nonperfusion, reduced density, and structural abnormalities[23,49-54], our findings may suggest that real-time imaging of retinal blood vessels could be useful in monitoring the progression of AD.

Supplementary Material

Refer to Web version on PubMed Central for supplementary material.

Acknowledgments:

We thank Jo Ann M. Eliason for help with manuscript editing. The authors dedicate the manuscript to the memory of Dr. Salomon Moni Hamaoui and Lillian Jones Black, who died of Alzheimer’s disease.

Funding sources:

Alzheimer's Association Research Fellowship to Promote Diversity AARFD-21-851509 (H.S.); National Institute on Aging (NIA) of the National Institutes of Health (NIH) R01 AG055865, R01 AG056478 and R01 AG075998 (M.K.H.); The Tom Gordon and The Haim Saban Private Foundations (M.K.H.); The Ray Charles Foundation (O.J.). National Eye Institute (NEI) of the NIH R01 EY013431 (A.V.L.). NIH P30 AG 066530 (D.H.).

REFERENCES

1. Attems J, Jellinger KA. The overlap between vascular disease and Alzheimer's disease--lessons from pathology. BMC Med. Nov 11 2014;12:206. doi:10.1186/s12916-014-0206-2 [PubMed: 25385447]
2. Arvanitakis Z, Leurgans SE, Wang Z, Wilson RS, Bennett DA, Schneider JA. Cerebral amyloid angiopathy pathology and cognitive domains in older persons. Ann Neurol. Feb 2011;69(2):320–7. doi:10.1002/ana.22112 [PubMed: 21387377]
3. Viswanathan A, Greenberg SM. Cerebral amyloid angiopathy in the elderly. Ann Neurol. Dec 2011;70(6):871–80. doi:10.1002/ana.22516 [PubMed: 22190361]
4. Biffi A, Greenberg SM. Cerebral amyloid angiopathy: a systematic review. J Clin Neurol. Mar 2011;7(1):1–9. doi:10.3988/jcn.2011.7.1.1 [PubMed: 21519520]
5. Weller RO, Subash M, Preston SD, Mazanti I, Carare RO. Perivascular drainage of amyloid-beta peptides from the brain and its failure in cerebral amyloid angiopathy and Alzheimer's disease. Brain Pathol. Apr 2008;18(2):253–66. doi:10.1111/j.1750-3639.2008.00133.x [PubMed: 18363936]
6. Hawkes CA, Jayakody N, Johnston DA, Bechmann I, Carare RO. Failure of perivascular drainage of beta-amyloid in cerebral amyloid angiopathy. Brain Pathol. Jul 2014;24(4):396–403. doi:10.1111/bpa.12159 [PubMed: 24946077]
7. Montagne A, Zhao Z, Zlokovic BV. Alzheimer's disease: A matter of blood-brain barrier dysfunction? J Exp Med. Nov 6 2017;214(11):3151–3169. doi:10.1084/jem.20171406 [PubMed: 29061693]
8. Mirzaei N, Shi H, Oviatt M, et al. Alzheimer’s Retinopathy: Seeing Disease in the Eyes. Review. Frontiers in Neuroscience. 2020-September-08 2020;14(921)doi:10.3389/fnins.2020.00921
9. Green AJ, McQuaid S, Hauser SL, Allen IV, Lyness R. Ocular pathology in multiple sclerosis: retinal atrophy and inflammation irrespective of disease duration. Brain. Jun 2010;133(Pt 6):1591–601. doi:10.1093/brain/awq080 [PubMed: 20410146]

10. Archibald NK, Clarke MP, Mosimann UP, Burn DJ. The retina in Parkinson's disease. Brain. May 2009;132(Pt 5):1128–45. doi:10.1093/brain/awp068 [PubMed: 19336464]
11. Du X, Koronyo Y, Mirzaei N, et al. Label-free hyperspectral imaging and deep-learning prediction of retinal amyloid beta-protein and phosphorylated tau. PNAS Nexus. Sep 2022;1(4):pgac164. doi:10.1093/pnasnexus/pgac164 [PubMed: 36157597]
12. Koronyo Y, Biggs D, Barron E, et al. Retinal amyloid pathology and proof-of-concept imaging trial in Alzheimer's disease. JCI Insight. Aug 17 2017;2(16)doi:10.1172/jci.insight.93621
13. Hadoux X, Hui F, Lim JKH, et al. Non-invasive in vivo hyperspectral imaging of the retina for potential biomarker use in Alzheimer's disease. Nat Commun. Sep 17 2019;10(1):4227. doi:10.1038/s41467-019-12242-1 [PubMed: 31530809]
14. Shi H, Koronyo Y, Rentsendorj A, et al. Retinal Vasculopathy in Alzheimer's Disease. Front Neurosci. 2021;15:731614. doi:10.3389/fnins.2021.731614 [PubMed: 34630020]
15. Bulut M, Kurtulus F, Gozkaya O, et al. Evaluation of optical coherence tomography angiographic findings in Alzheimer's type dementia. Br J Ophthalmol. Feb 2018;102(2):233–237. doi:10.1136/bjophthalmol-2017-310476 [PubMed: 28600299]
16. Snyder PJ, Alber J, Alt C, et al. Retinal imaging in Alzheimer's and neurodegenerative diseases. Alzheimers Dement. Jan 2021;17(1):103–111. doi:10.1002/alz.12179 [PubMed: 33090722]
17. Koronyo-Hamaoui M, Koronyo Y, Ljubimov AV, et al. Identification of amyloid plaques in retinas from Alzheimer's patients and noninvasive in vivo optical imaging of retinal plaques in a mouse model. Neuroimage. Jan 2011;54 Suppl 1:S204–17. doi:10.1016/j.neuroimage.2010.06.020 [PubMed: 20550967]
18. den Haan J, Morrema THJ, Verbraak FD, et al. Amyloid-beta and phosphorylated tau in post-mortem Alzheimer's disease retinas. Acta Neuropathol Commun. Dec 28 2018;6(1):147. doi:10.1186/s40478-018-0650-x [PubMed: 30593285]
19. Hinton DR, Sadun AA, Blanks JC, Miller CA. Optic-nerve degeneration in Alzheimer's disease. N Engl J Med. Aug 21 1986;315(8):485–7. doi:10.1056/NEJM198608213150804 [PubMed: 3736630]
20. Koronyo Y, Salumbides BC, Black KL, Koronyo-Hamaoui M. Alzheimer's disease in the retina: imaging retinal abeta plaques for early diagnosis and therapy assessment. Neurodegener Dis. 2012;10(1–4):285–93. doi:10.1159/000335154 [PubMed: 22343730]
21. Xu QA, Boerkoel P, Hirsch-Reinshagen V, et al. Muller cell degeneration and microglial dysfunction in the Alzheimer's retina. Acta Neuropathol Commun. Oct 5 2022;10(1):145. doi:10.1186/s40478-022-01448-y [PubMed: 36199154]
22. Hart de Ruyter FJ, Morrema THJ, den Haan J, et al. Phosphorylated tau in the retina correlates with tau pathology in the brain in Alzheimer's disease and primary tauopathies. Acta Neuropathol. Dec 8 2022;doi:10.1007/s00401-022-02525-1
23. Shi H, Koronyo Y, Rentsendorj A, et al. Identification of early pericyte loss and vascular amyloidosis in Alzheimer's disease retina. Acta Neuropathol. May 2020;139(5):813–836. doi:10.1007/s00401-020-02134-w [PubMed: 32043162]
24. Singer MB, Ringman JM, Chu Z, et al. Abnormal retinal capillary blood flow in autosomal dominant Alzheimer's disease. Alzheimers Dement (Amst). 2021;13(1):e12162. doi:10.1002/dad2.12162 [PubMed: 33728371]
25. Shi H, Koronyo Y, Fuchs DT, et al. Retinal capillary degeneration and blood-retinal barrier disruption in murine models of Alzheimer's disease. Acta Neuropathol Commun. Nov 23 2020;8(1):202. doi:10.1186/s40478-020-01076-4 [PubMed: 33228786]
26. Perez-Riverol Y, Bai J, Bandla C, et al. The PRIDE database resources in 2022: a hub for mass spectrometry-based proteomics evidences. Nucleic Acids Res. Jan 7 2022;50(D1):D543–D552. doi:10.1093/nar/gkab1038 [PubMed: 34723319]
27. Giebel SJ, Menicucci G, McGuire PG, Das A. Matrix metalloproteinases in early diabetic retinopathy and their role in alteration of the blood-retinal barrier. Lab Invest. May 2005;85(5):597–607. doi:10.1038/labinvest.3700251 [PubMed: 15711567]
28. Greene C, Hanley N, Campbell M. Claudin-5: gatekeeper of neurological function. Fluids Barriers CNS. Jan 29 2019;16(1):3. doi:10.1186/s12987-019-0123-z [PubMed: 30691500]

29. Van Itallie CM, Tietgens AJ, Anderson JM. Visualizing the dynamic coupling of claudin strands to the actin cytoskeleton through ZO-1. Mol Biol Cell. Feb 15 2017;28(4):524–534. doi:10.1091/mbc.E16-10-0698 [PubMed: 27974639]
30. Fanning AS, Jameson BJ, Jesaitis LA, Anderson JM. The tight junction protein ZO-1 establishes a link between the transmembrane protein occludin and the actin cytoskeleton. J Biol Chem. Nov 6 1998;273(45):29745–53. doi:10.1074/jbc.273.45.29745 [PubMed: 9792688]
31. Laver NM, Robison WG Jr., Pfeffer BA. Novel procedures for isolating intact retinal vascular beds from diabetic humans and animal models. Invest Ophthalmol Vis Sci. May 1993;34(6):2097–104. [PubMed: 8491560]
32. Veenstra A, Liu H, Lee CA, Du Y, Tang J, Kern TS. Diabetic Retinopathy: Retina-Specific Methods for Maintenance of Diabetic Rodents and Evaluation of Vascular Histopathology and Molecular Abnormalities. Curr Protoc Mouse Biol. Sep 1 2015;5(3):247–270. doi:10.1002/9780470942390.mo140190 [PubMed: 26331759]
33. Roy S, Ha J, Trudeau K, Beglova E. Vascular basement membrane thickening in diabetic retinopathy. Curr Eye Res. Dec 2010;35(12):1045–56. doi:10.3109/02713683.2010.514659 [PubMed: 20929292]
34. Yamazaki Y, Kanekiyo T. Blood-Brain Barrier Dysfunction and the Pathogenesis of Alzheimer's Disease. Int J Mol Sci. Sep 13 2017;18(9)doi:10.3390/ijms18091965
35. Diaz-Coranguez M, Ramos C, Antonetti DA. The inner blood-retinal barrier: Cellular basis and development. Vision Res. Oct 2017;139:123–137. doi:10.1016/j.visres.2017.05.009 [PubMed: 28619516]
36. Lampugnani MG. Endothelial cell-to-cell junctions: adhesion and signaling in physiology and pathology. Cold Spring Harb Perspect Med. Oct 1 2012;2(10)doi:10.1101/cshperspect.a006528
37. Carrano A, Hoozemans JJ, van der Vies SM, van Horssen J, de Vries HE, Rozemuller AJ. Neuroinflammation and blood-brain barrier changes in capillary amyloid angiopathy. Neurodegener Dis. 2012;10(1–4):329–31. doi:10.1159/000334916 [PubMed: 22301467]
38. Carrano A, Hoozemans JJ, van der Vies SM, Rozemuller AJ, van Horssen J, de Vries HE. Amyloid Beta induces oxidative stress-mediated blood-brain barrier changes in capillary amyloid angiopathy. Antioxid Redox Signal. Sep 1 2011;15(5):1167–78. doi:10.1089/ars.2011.3895 [PubMed: 21294650]
39. Park SW, Kim JH, Mook-Jung I, et al. Intracellular amyloid beta alters the tight junction of retinal pigment epithelium in 5XFAD mice. Neurobiol Aging. Sep 2014;35(9):2013–20. doi:10.1016/j.neurobiolaging.2014.03.008 [PubMed: 24709310]
40. Shi H, Yin Z, Koronyo Y, et al. Regulating microglial miR-155 transcriptional phenotype alleviates Alzheimer's-induced retinal vasculopathy by limiting Clec7a/Galectin-3(+) neurodegenerative microglia. Acta Neuropathol Commun. Sep 8 2022;10(1):136. doi:10.1186/s40478-022-01439-z [PubMed: 36076283]
41. Gireud-Goss M, Mack AF, McCullough LD, Urayama A. Cerebral Amyloid Angiopathy and Blood-Brain Barrier Dysfunction. Neuroscientist. Dec 2021;27(6):668–684. doi:10.1177/1073858420954811 [PubMed: 33238806]
42. Magaki S, Tang Z, Tung S, et al. The effects of cerebral amyloid angiopathy on integrity of the blood-brain barrier. Neurobiol Aging. Oct 2018;70:70–77. doi:10.1016/j.neurobiolaging.2018.06.004 [PubMed: 30007166]
43. Sprague AH, Khalil RA. Inflammatory cytokines in vascular dysfunction and vascular disease. Biochem Pharmacol. Sep 15 2009;78(6):539–52. doi:10.1016/j.bcp.2009.04.029 [PubMed: 19413999]
44. Fahey E, Doyle SL. IL-1 Family Cytokine Regulation of Vascular Permeability and Angiogenesis. Front Immunol. 2019;10:1426. doi:10.3389/fimmu.2019.01426 [PubMed: 31293586]
45. Grimaldi A, Pediconi N, Oieni F, et al. Neuroinflammatory Processes, A1 Astrocyte Activation and Protein Aggregation in the Retina of Alzheimer's Disease Patients, Possible Biomarkers for Early Diagnosis. Front Neurosci. 2019;13:925. doi:10.3389/fnins.2019.00925 [PubMed: 31551688]
46. Ning A, Cui J, To E, Ashe KH, Matsubara J. Amyloid-beta deposits lead to retinal degeneration in a mouse model of Alzheimer disease. Invest Ophthalmol Vis Sci. Nov 2008;49(11):5136–43. doi:10.1167/iovs.08-1849 [PubMed: 18566467]

47. Yamada M Cerebral amyloid angiopathy: an overview. Neuropathology. Mar 2000;20(1):8–22. doi:10.1046/j.1440-1789.2000.00268.x [PubMed: 10935432]

48. Paton D, Duke JR. Primary familial amyloidosis. Ocular manifestations with histopathologic observations. Am J Ophthalmol. Apr 1966;61(4):736–47. [PubMed: 5931270]

49. Frost S, Kanagasingam Y, Sohrabi H, et al. Retinal vascular biomarkers for early detection and monitoring of Alzheimer's disease. Transl Psychiatry. Feb 26 2013;3:e233. doi:10.1038/tp.2012.150 [PubMed: 23443359]

50. O'Bryhim BE, Apte RS, Kung N, Coble D, Van Stavern GP. Association of Preclinical Alzheimer Disease With Optical Coherence Tomographic Angiography Findings. JAMA Ophthalmol. Nov 1 2018;136(11):1242–1248. doi:10.1001/jamaophthalmol.2018.3556 [PubMed: 30352114]

51. Cabrera DeBuc D, Somfai GM, Arthur E, Kostic M, Oropesa S, Mendoza Santiesteban C. Investigating Multimodal Diagnostic Eye Biomarkers of Cognitive Impairment by Measuring Vascular and Neurogenic Changes in the Retina. Front Physiol. 2018;9:1721. doi:10.3389/fphys.2018.01721 [PubMed: 30574092]

52. Csincsik L, MacGillivray TJ, Flynn E, et al. Peripheral Retinal Imaging Biomarkers for Alzheimer's Disease: A Pilot Study. Ophthalmic Res. 2018;59(4):182–192. doi:10.1159/000487053 [PubMed: 29621759]

53. Berisha F, Feke GT, Trempe CL, McMeel JW, Schepens CL. Retinal abnormalities in early Alzheimer's disease. Invest Ophthalmol Vis Sci. May 2007;48(5):2285–9. doi:10.1167/iovs.06-1029 [PubMed: 17460292]

54. Abbasi J. A Retinal Scan for Alzheimer Disease. JAMA. Oct 10 2017;318(14):1314. doi:10.1001/jama.2017.15192

Systematic review:

We reviewed the literature using traditional PubMed sources and meeting abstracts. Previous studies demonstrated blood-brain barrier damage and intense arteriolar beta-amyloid (Aβ) accumulation in the brains of patients with Alzheimer's disease (AD). An earlier investigation by our team revealed retinal vascular pericyte loss and amyloidosis, yet how AD affects retinal blood vessels and the blood-retinal barrier (BRB) continues to be unknown. Relevant citations are cited.

Interpretation:

Our analyses indicate tight junction loss in the inner BRB and intense arteriolar $A\beta_{40}$ deposition in AD patients—retinal vascular biomarkers significantly associated with cerebral amyloid angiopathy (CAA) and other brain neuropathology. Our discoveries are consistent with previous findings in the brains and retinas of AD patients.

Future directions:

The current study identified retinal vascular alterations in AD patients and incentivizes us to conduct future retinal imaging studies to confirm these findings as well as assess correlations with CAA and cognitive deficit.

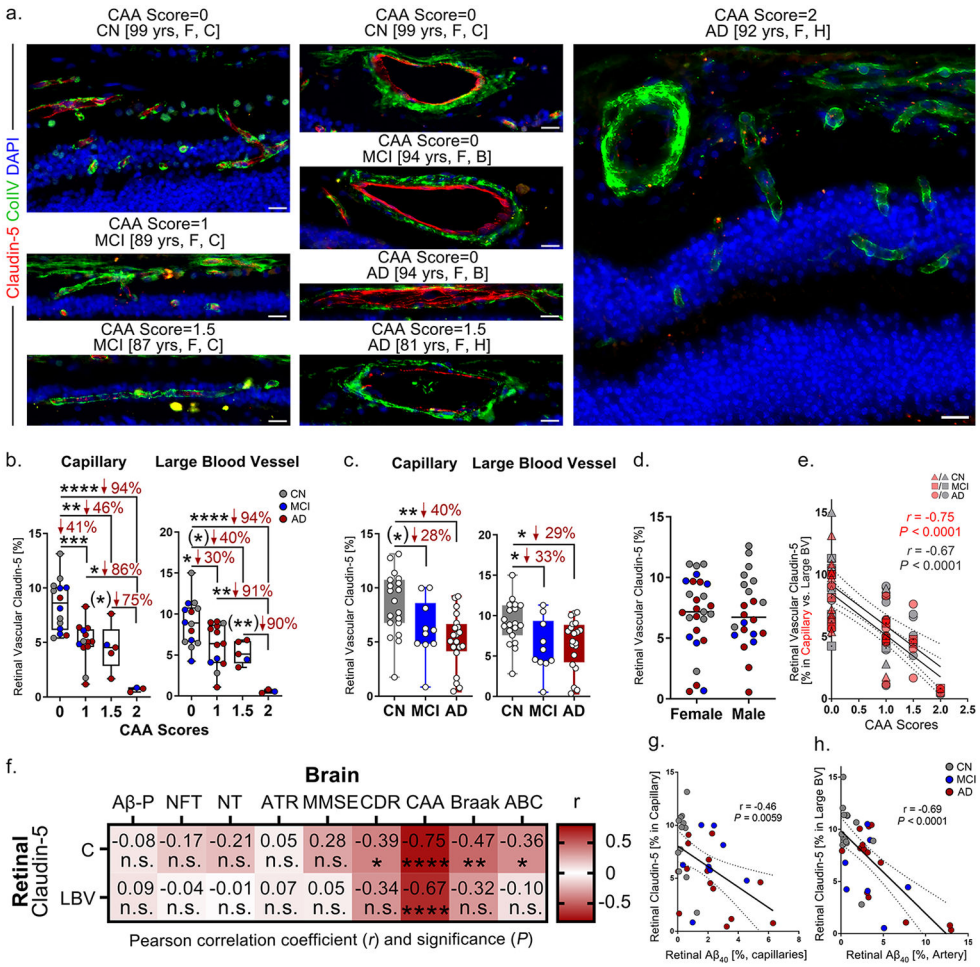

Figure 1.

Loss of retinal endothelial claudin-5 in MCI and AD patients in relation to retinal vascular amyloidosis, CAA and cognitive deficit.

a. Representative images of immunofluorescent staining for claudin-5 (red), collagen IV (ColIV, green), and DAPI (blue) on postmortem cross-sections of retina from cognitively normal (CN, n=21 [control]) patients as well as from patients with mild cognitive impairment (MCI, n=10) and those with Alzheimer's disease (AD, n=21) with different degrees of CAA severity scores. Abbreviations: yrs, years old; F, female; C, Caucasian; B, Black; H, Hispanic. All scale bars=20μm.

b-c. Quantitative analysis of retinal vascular claudin-5 immunoreactivity (IR) separately in capillaries and large blood vessels (LBVs) from all experimental groups stratified by **b.** CAA severity scores and by **c.** diagnostic groups (n=53 in total).

d. Average of retinal vascular claudin-5 immunoreactivity (IR) in capillaries and LBVs stratified by sex in the same cohort (n=53 total).

e. Pearson's coefficient (r) correlation between CAA severity scores and claudin-5 in retinal capillaries (red) and LBVs (gray) (n=35 total).

f. Heatmaps illustrating Pearson's correlations between retinal claudin-5 in capillaries and LBVs versus brain pathology and cognitive decline, including Aβ plaques (Aβ-P),

neurofibrillary tangles (NFT), neuropil threads (NT), atrophy (ATR), Mini-Mental State Examination (MMSE) scores, Clinical Dementia Rating (CDR) scores, CAA severity scores, Braak stages, and A (amyloid) B (Braak) C (CERAD) average scores in AD (n=18), MCI (n=10) and CN (n=9) human donors (n=37 total). Pseudo-color red and numbers demonstrate the strength of (r) correlation power; statistical significance is demonstrated as follows: n.s., not significant, *$p < 0.05$, **$p < 0.01$, ****$p < 0.0001$.

g-h. Pearson's coefficient (r) correlation between **g.** retinal $A\beta_{40}$ versus claudin-5 in capillaries and **h.** retinal arteriolar $A\beta_{40}$ versus claudin-5 in LBVs.

Data from individual donors (circles) as well as group means ± SEMs are shown. *$p < 0.05$, **$p < 0.01$, ***$p < 0.001$, ****$p < 0.0001$, by one-way ANOVA with Tukey's post-hoc multiple comparison test. Two-group statistical analysis was performed using an unpaired two-tailed Student t-test, and results are shown in parentheses. Percentage decreases are shown in red.

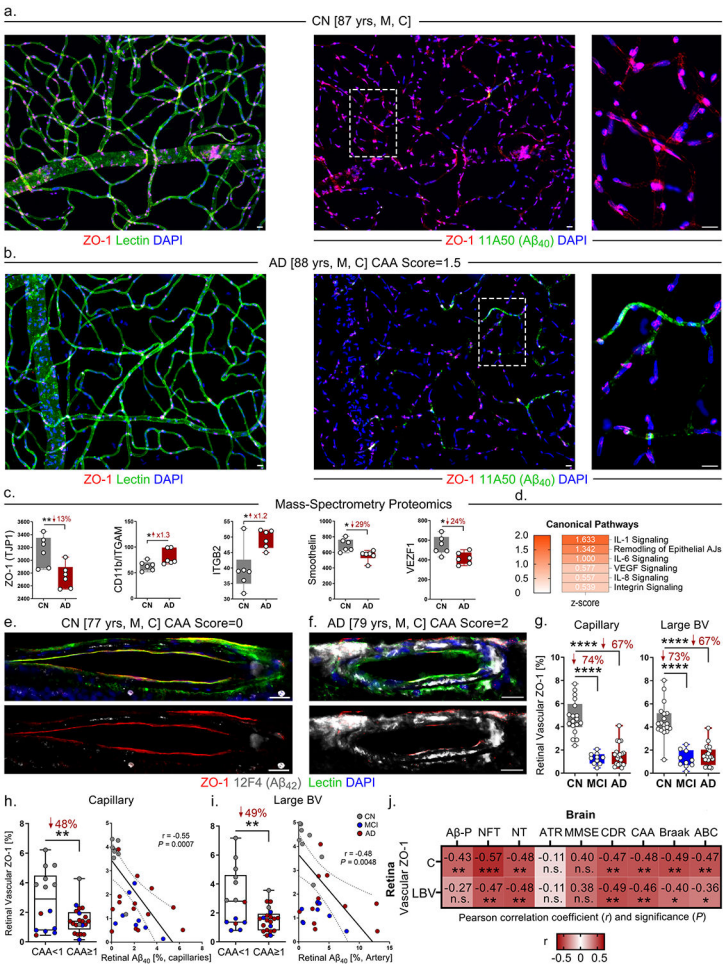

Figure 2.

Significant association between retinal vascular ZO-1 deficiency and multiple cerebral neuropathology and cognitive status in MCI and AD patients.

a-b. Representative images of immunofluorescent staining for ZO-1 (red), lectin for blood vessels (green), and DAPI (blue) on isolated postmortem retinal blood vessels from an AD patient versus an age and sex-matched CN control. Abbreviations: yrs, years old; M, male; C, Caucasian. All scale bars=20μm. Right panels are zoomed-in images from regions surrounded by dashed lines.

c. Mass-spectrometry proteomic analyses for protein expression of ZO-1, CD11b/ITGAM, ITGB2, smoothelin, and VEZF1 in postmortem retinal lysates from a cohort of AD patients (n=6) and CN controls (n=6).

d. Ingenuity Pathway Analyses (IPA) with z-scores for canonical pathways including IL-1, IL-6, VEGF, IL-8, and integrin signaling, and remodeling of epithelial adherens junctions (AJs) in the same cohort (n=12 total).

e-f. Representative images of immunofluorescent staining for ZO-1 (red), 12F4 ($A\beta_{42}$, white), lectin (green), and DAPI (blue) on postmortem retinal cross-sections from MCI (n=10) and AD (n=21) patients versus CN controls (n=22). Abbreviations: yrs, years old; M, male; C, Caucasian. All scale bars=20μm.

g. Quantitative analysis of retinal vascular ZO-1 immunoreactivity (IR) separately in capillaries and large blood vessels (BVs) from all experimental groups of the same cohort (n=53 total).

h. Quantitative analysis of retinal ZO-1 IR in capillaries stratified by CAA severity scores <1 versus ≥1 (left panel). Pearson's coefficient (r) correlation between retinal $A\beta_{40}$ versus ZO-1 in capillaries (right panel).

i. Quantitative analysis of retinal ZO-1 IR in large BVs stratified by CAA severity scores <1 versus ≥1 (left panel). Pearson's coefficient (r) correlation between retinal arteriolar $A\beta_{40}$ versus ZO-1 in large BVs (right panel).

j. Heatmaps illustrating Pearson's correlations between retinal ZO-1 in capillaries and large BVs versus brain pathology and cognitive decline, including Aβ plaques (Aβ-P), neurofibrillary tangles (NFT), neuropil threads (NT), atrophy (ATR), MMSE scores, CDR scores, CAA severity scores, Braak stages, and A (Amyloid) B (Braak) C (CERAD) average scores in AD (n=18), MCI (n=10), and CN (n=9) human donors (n=37 total). Pseudo-color red and numbers demonstrate the strength of (r) correlation power; statistical significance is demonstrated as follows: n.s., not significant, $*p < 0.05$, $**p < 0.01$, $***p < 0.001$.

Data from individual donors (circles) as well as group means ± SEMs are shown. $*p < 0.05$, $**p < 0.01$, $****p < 0.0001$, by one-way ANOVA with Tukey's post-hoc multiple comparison test for three group analyses. Two group statistical analysis was performed using an unpaired two-tailed Student t-test. Fold changes and percentage decreases are shown in red.

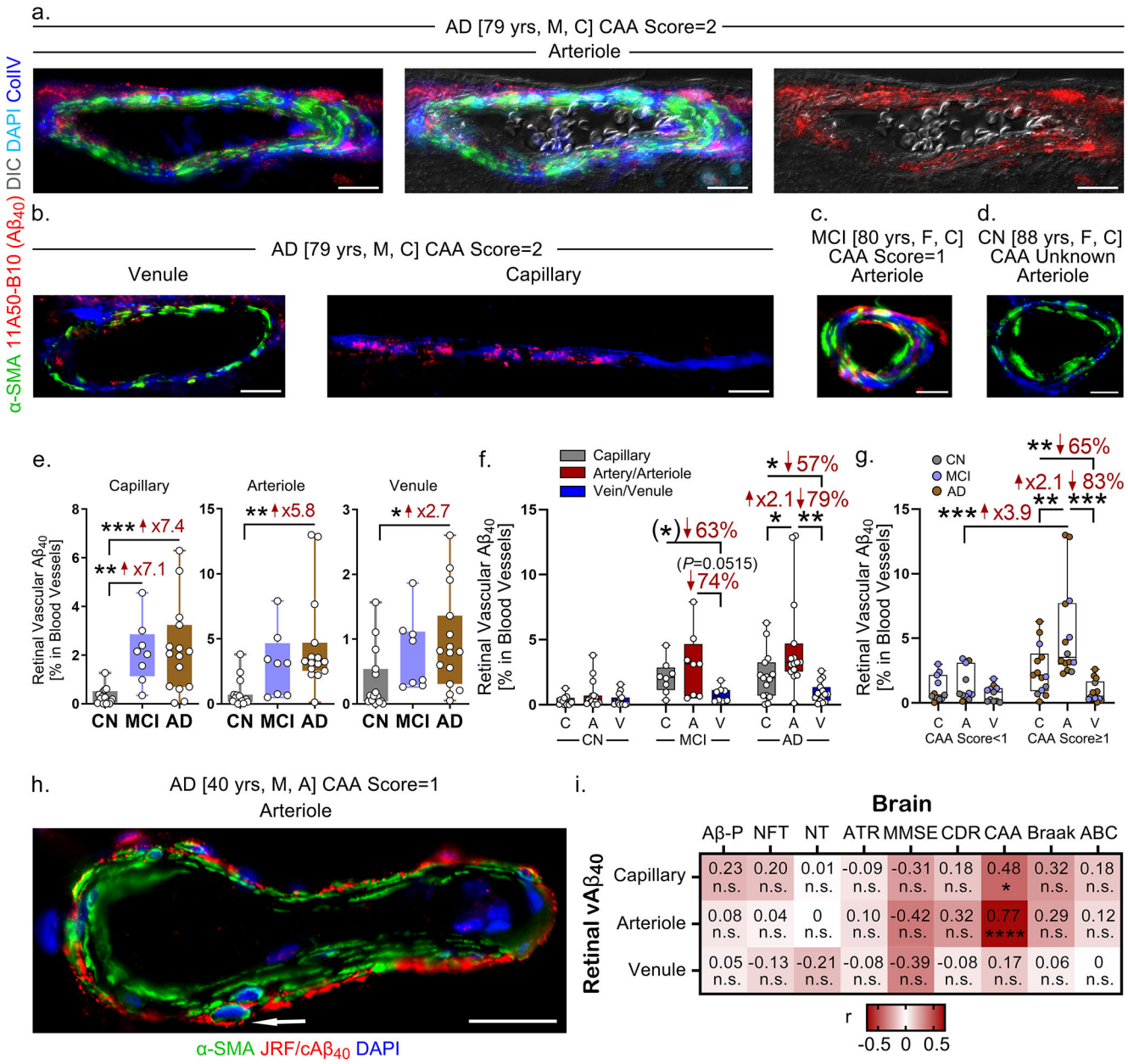

Figure 3.

Intense retinal arteriolar $A\beta_{40}$ accumulation tightly associated with CAA severity scores in MCI and AD patients.

a-d. Representative images of immunofluorescent staining for 11A50-B10 ($A\beta_{40}$, red) in various retinal blood vessel types, α-SMA (green), collagen IV (ColIV, blue), and DAPI (cyan) with a differential interference contrast (DIC) channel on postmortem retinal cross-sections from MCI (n=8) and AD (n=15) patients versus CN controls (n=15). Abbreviations: yrs, years old; M, male; F, female; C, Caucasian. All scale bars=20μm.

e. Quantitative analysis of retinal vascular $A\beta_{40}$ immunoreactivity (IR) by 11A50-B10 in retinal blood vessel types—capillaries, arterioles, and venules—stratified by diagnostic groups of the same cohort (n=38 total).

f. Quantitative analysis of retinal vascular $A\beta_{40}$ IR stratified by blood vessel type and diagnostic group in the same cohort (n=38 total).

g. Quantitative analysis of retinal vascular $A\beta_{40}$ IR stratified by blood vessel type and CAA severity score <1 versus ≥1 in the same cohort (n=38 total).

h. Representative image of immunofluorescent staining for arteriolar JRF/c$A\beta_{40}$ ($A\beta_{40}$, red), α-SMA (green), and DAPI (blue) on postmortem retinal cross-sections from an AD patient. Abbreviations: yrs, years old; M, male; A, Asian. Scale bar=20μm. Arrow indicates $A\beta_{40}$ accumulation in a smooth muscle cell.

i. Heatmaps illustrating Pearson's correlations between retinal $A\beta_{40}$ by 11A50-B10 in capillaries, arterioles, and venules versus brain pathology and cognitive decline, including Aβ plaques (Aβ-P), neurofibrillary tangles (NFT), neuropil threads (NT), atrophy (ATR), MMSE scores, CDR scores, CAA severity scores, Braak stages, and A (Amyloid) B (Braak) C (CERAD) average scores in AD (n=14), MCI (n=8) and CN (n=12) human donors (n=34 total). Pseudo-color red and numbers demonstrate the strength of (r) correlation power; statistical significance is demonstrated as follows: n.s., not significant, $*p < 0.05$, $****p < 0.0001$.

Data from individual donors (circles) as well as group means ± SEMs are shown. $*p < 0.05$, $**p < 0.01$, $***p < 0.001$ by two-way or one-way ANOVA with Tukey's post-hoc multiple comparison test. Two group statistical analysis was performed using an unpaired two-tailed Student t-test and is shown in parentheses. Fold changes and percentage decreases are shown in red.

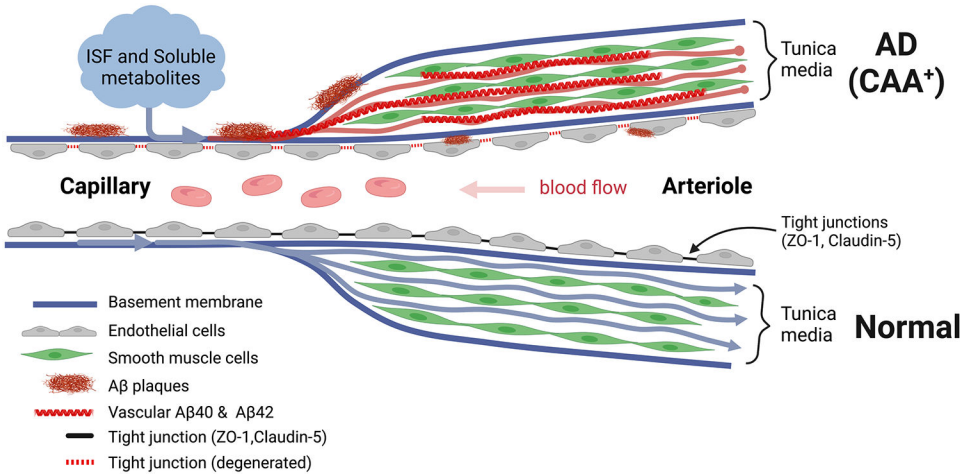

Figure 4.

Graphic illustration describing failure of drainage of Aβ plaques through the intramural peri-arterial drainage (IPAD) system, which results in accumulation of Aβ in retinal arterioles and capillaries. A pathological IPAD system with degenerating tight junctions of retinal endothelium from AD patients with cerebral amyloid angiopathy (CAA) is shown in comparison with a normal healthy control. Abbreviation: ISF, interstitial fluid. This illustration was created by using Biorender.com.

Table 1.

Demographic, clinical, and neuropathological data on human donors included in the immunohistochemical analyses

		CN	MCI	AD	F	*P*
IHC (n=53)		**22** (11F, 11M)	**10** (6F, 4M)	**21** (11F, 10M)	-	-
Age at death (Years)		**82.1 ± 10.9**	**88.7 ± 5.7**	**85.6 ± 8.5**	1.89	*0.16*
Race (no.)		W(18); H(3); B(1)	W(8); H(1); B(1)	W(13); H(4); B(1); A (1); n.a. (2)	-	-
PMI (hours)		7.5 ± 4.0	8.3 ± 5.2	8.4 ± 4.9	0.18	*0.84*
MMSE score (n=15)		27.5 ± 2.9	23.5 ± 2.1	13.6 ± 8.8	8.86	***0.0043***
CDR score (n=29)		0.2 ± 0.4	1.5 ± 1.4	2.3 ± 1.0	8.019	***0.0019***
Brain neuropathology (severity score [n=38])	**Braak stage**	I-II (56%) III-IV (33%) V-VI (11%)	I-II (30%) III-IV (40%) V-VI (30%)	I-II (5%) III-IV (21%) V-VI (74%)	9.50	***0.0005***
	ABC (amyloid, Braak, CERAD)	1.93 ± 0.71	2.17 ± 0.58	2.74 ± 0.35	8.24	***0.0013***
	Aβ plaque	1.29 ± 1.20	2.00 ± 1.03	2.58 ± 0.98	4.71	***0.0154***
	NFTs	0.55 ± 0.55	1.78 ± 0.99	2.21 ± 0.96	10.70	***0.0002***
	NTs	0.49 ± 0.88	1.17 ± 0.75	1.92 ± 1.05	7.34	***0.0022***
	Atrophy	0.96 ± 1.02	1.11 ± 1.01	1.56 ± 0.94	1.42	*0.2544*

List of human donors (total N=53 subjects) included in histological analyses. IHC, immunohistochemistry; CN, cognitively normal; MCI, mild cognitive impairment; AD, Alzheimer's disease; F, female, M, male; SD, standard deviation; W, White; B, Black; H, Hispanic; A, Asian; PMI, post-mortem interval; MMSE, Mini-Mental State Examination; CDR, Clinical dementia rating; n.a., not available. Paired brains with full neuropathological assessments were available for 38 human donors; Aβ, Amyloid-β protein; NFTs, neurofibrillary tangles; NTs, neuropil threads; Mean ABC scores were determined as follows: A, Aβ plaque score modified from Thal; B, NFT stage modified from Braak; C, Neuritic plaque score modified from CERAD. Group values are presented as mean ± standard deviation. F and *P* values were determined using one-way ANOVA with Tukey's multiple comparisons test. *P* values presented in bold type demonstrate significance.

Table 2.

Demographic, clinical, and neuropathological data on human donors included in the mass-spectrometry proteomic analyses

		CN	AD	*t*	*P*
Mass spectrometry (n=12)		**6** (3F, 3M)	**6** (4F, 2M)	-	-
Age at death (years)		**76.8 ± 5.9**	**82.5 ± 19.4**	0.68	*0.52*
Race (no.)		W(5); H(1)	W(4); B(1); H(1)	-	-
PMI (hours)		9.0 ± 5.1	7.3 ± 2.7	0.62	*0.57*
MMSE score (n=3)		23.0 ± n.a.	17.0 ± 1.4	-	-
CDR score (n=6)		0.25 ± 0.35	2.25 ± 0.96	2.72	*0.053*
Brain neuropathology (severity score [n=8])	**Braak stage**	I-II (100%)	V-VI (100%)	31.03	***<0.0001***
	ABC (amyloid, Braak, CERAD)	1.83 ± 0.71	2.67 ± 0.27	1.61	*0.33*
	Aβ plaque	1.76 ± 0.68	3.09 ± 1.26	1.90	*0.14*
	NFTs	1.15 ± 0.01	2.50 ± 0.96	3.45	***0.0182***
	NTs	0.22 ± 0.11	1.43 ± 0.43	5.91	***0.0022***
	Atrophy	0.55 ± 0.07	1.41 ± 0.97	2.16	*0.08*

List of human donors (total N=12 subjects) included in protein analyses. CN, cognitively normal; AD, Alzheimer's disease; F, female, M, male; W, White; B, Black; H, Hispanic; PMI, post-mortem interval; MMSE, Mini-Mental State Examination; CDR, Clinical dementia rating; n.a., not available. Paired brains with full neuropathological assessments were available for eight human donors; Aβ, Amyloid-β protein; NFTs, neurofibrillary tangles; NTs, neuropil threads; Mean ABC scores were determined as follows: A, Aβ plaque score modified from Thal; B, NFT stage modified from Braak; C, Neuritic plaque score modified from CERAD. Group values are presented as mean ± standard deviation. *t* and *P* values were determined using an unpaired Student's t-test. *P* values presented in bold type demonstrate significance.